Discover 25+ Color Optimized Flow Cytometry Panels
- Human General Phenotyping Panel
- Human T Cell Differentiation and Exhaustion Panel
- Human T Cell Differentiation and CCRs Panel
Learn more
BioLegend®

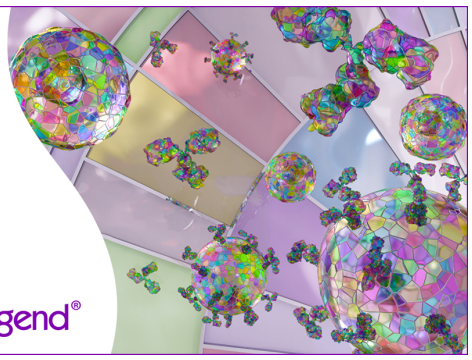

The Journal of Immunology
RESEARCH ARTICLE | DECEMBER 15 2011

Cannabinoid Receptor Type 1 Protects Nigrostriatal Dopaminergic Neurons against MPTP Neurotoxicity by Inhibiting Microglial Activation FREE

Young C. Chung; ... et. al

J Immunol (2011) 187 (12): 6508–6517.
https://doi.org/10.4049/jimmunol.1102435

Related Content

Ethyl Pyruvate Rescues Nigrostriatal Dopaminergic Neurons by Regulating Glial Activation in a Mouse Model of Parkinson's Disease
J Immunol (July,2011)

Paroxetine Prevents Loss of Nigrostriatal Dopaminergic Neurons by Inhibiting Brain Inflammation and Oxidative Stress in an Experimental Model of Parkinson's Disease
J Immunol (July,2010)

Induction of Adaptive Immunity Leads to Nigrostriatal Disease Progression in MPTP Mouse Model of Parkinson's Disease
J Immunol (June,2017)

Downloaded from http://journals.aai.org/jimmunol/article-pdf/187/12/6508/1342902/1102435.pdf by guest on 19 April 2024

Cannabinoid Receptor Type 1 Protects Nigrostriatal Dopaminergic Neurons against MPTP Neurotoxicity by Inhibiting Microglial Activation

Young C. Chung,*,†,[1] Eugene Bok,*,†,[2] Sue H. Huh,*,†,‡,§ Ju-Young Park,¶ Sung-Hwa Yoon,¶ Sang R. Kim,*,† Yoon-Seong Kim,‖ Sungho Maeng,# Sung Hyun Park,# and Byung K. Jin*

This study examined whether the cannabinoid receptor type 1 (CB_1) receptor contributes to the survival of nigrostriatal dopaminergic (DA) neurons in the 1-methyl-4-phenyl-1,2,3,6-tetrahydropyridine (MPTP) mouse model of Parkinson's disease. MPTP induced significant loss of nigrostriatal DA neurons and microglial activation in the substantia nigra (SN), visualized with tyrosine hydroxylase or macrophage Ag complex-1 immunohistochemistry. Real-time PCR, ELISA, Western blotting, and immunohistochemistry disclosed upregulation of proinflammatory cytokines, activation of microglial NADPH oxidase, and subsequent reactive oxygen species production and oxidative damage of DNA and proteins in MPTP-treated SN, resulting in degeneration of DA neurons. Conversely, treatment with nonselective cannabinoid receptor agonists (WIN55,212-2 and HU210) led to increased survival of DA neurons in the SN, their fibers and dopamine levels in the striatum, and improved motor function. This neuroprotection by cannabinoids was accompanied by suppression of NADPH oxidase reactive oxygen species production and reduced expression of proinflammatory cytokines from activated microglia. Interestingly, cannabinoids protected DA neurons against 1-methyl-4-phenyl-pyridinium neurotoxicity in cocultures of mesencephalic neurons and microglia, but not in neuron-enriched mesencephalic cultures devoid of microglia. The observed neuroprotection and inhibition of microglial activation were reversed upon treatment with CB_1 receptor selective antagonists AM251 and/or SR14,716A, confirming the involvement of the CB_1 receptor. The present in vivo and in vitro findings clearly indicate that the CB_1 receptor possesses anti-inflammatory properties and inhibits microglia-mediated oxidative stress. Our results collectively suggest that the cannabinoid system is beneficial for the treatment of Parkinson's disease and other disorders associated with neuroinflammation and microglia-derived oxidative damage. ***The Journal of Immunology*****, 2011, 187: 6508–6517.**

Parkinson's disease (PD) is a common neurodegenerative disorder characterized by the progressive degeneration of nigrostriatal dopaminergic (DA) neurons. The most prominent biochemical changes in PD involve reduction of the striatal dopamine levels that may result in abnormal motor behavior, including resting tremor, rigidity, and bradykinesia (1, 2). Although the specific cause of PD is yet to be established, a growing body of evidence supports the theory that microglial activation-derived oxidative stress increases the risk of PD (3). In the substantia nigra (SN) of PD patients and 1-methyl-4-phenyl-1,2,3,6-tetrahydropyridine (MPTP) models of PD, key enzymes involved in reactive oxygen species (ROS) production, such as microglial NAPDH oxidase, are upregulated in damaged areas and contribute to DA neuronal death (4–7). In addition, proinflammatory cytokines, such as IL-1β and TNF-α, are augmented in PD patients (8, 9) and participate in DA neuronal death in the MPTP model of PD (10, 11).

The cannabinoid receptor type 1 (CB_1) receptor is a member of the seven-transmembrane domain G-protein–coupled receptor family (12, 13). CB_1 receptor is primarily expressed in glutamatergic neurons and axon terminals of GABA interneurons in CNS (14). CB_1 receptor is also found in DA neurons (15) and

*Department of Biochemistry and Molecular Biology, School of Medicine, Kyung Hee University, Seoul 130-701, Korea; †Neurodegeneration Control Research Center, School of Medicine, Kyung Hee University, Seoul 130-701, Korea; ‡Neuroscience Graduate Program, School of Medicine, Ajou University, Suwon 443-479, Korea; §Division of Cell Transformation and Restoration, School of Medicine, Ajou University, Suwon 443-479, Korea; ¶Department of Molecular Science and Technology, Ajou University, Suwon 443-479, Korea; ‖Burnett School of Biomedical Sciences, College of Medicine, University of Central Florida, Orlando, FL 32827; and #Department of East-West Medicine, Graduate School of East-West Medical Science, Kyung Hee University, Yongin 446-701, Korea

[1]Current address: Laboratory of Neurobiology and Genetics, The Rockefeller University, New York, NY.

[2]Current address: Burnett School of Biomedical Sciences, College of Medicine, University of Central Florida, Orlando, FL.

Received for publication August 22, 2011. Accepted for publication October 4, 2011.

This work was supported by the Basic Science Research Program through the National Research Foundation of Korea funded by the Ministry of Education, Science, and Technology (Grant 20090063274).

Address correspondence and reprint requests to Prof. Byung K. Jin, Department of Biochemistry and Molecular Biology, Neurodegeneration Control Research Center, School of Medicine, Kyung Hee University, Seoul 130–701, South Korea. E-mail address: bkjin@khu.ac.kr

The online version of this article contains supplemental material.

Abbreviations used in this article: AEA, arachidonylethanolamide; CB_1, cannabinoid receptor type 1; CB_2, cannabinoid receptor type 2; Ct, threshold cycle; DA, dopaminergic; DIV, days in vitro; DNPH, 2,4-dinitrophenylhydrazine; MAC-1, macrophage Ag complex-1; MPP^+, 1-methyl-4-phenyl-pyridinium; MPTP, 1-methyl-4-phenyl-1,2,3,6-tetrahydropyridine; 6-OHDA, 6-hydroxydopmaine; 8-OHdG, 8-hydroxy-2'-deoxyguanosine; PB, phosphate buffer; PD, Parkinson's disease; ROS, reactive oxygen species; RT, room temperature; SN, substantia nigra; STR, striatum; TH, tyrosine hydroxylase.

Copyright © 2011 by The American Association of Immunologists, Inc. 0022-1767/11/$16.00

Downloaded from http://journals.aai.org/jimmunol/article-pdf/187/12/6508/1342902/1102435.pdf by guest on 19 April 2024

nonneuronal cells, including microglia (16), astrocytes (17, 18), and oligodendrocytes (19). This receptor is activated in response to endogenous ligands, which are mainly derivatives of polyunsaturated fatty acids, including anandamide (arachidonylethanolamide [AEA]) (20, 21) and 2-arachidonoylglycerol (21, 22). Several synthetic cannabinoids, such as HU210 (23, 24) and WIN55,212-2 (24, 25), have been confirmed as ligands of the CB_1 receptor. However, the effects of endogenous and synthetic cannabinoids differ (26).

Autoradiography, in situ hybridization (27), and immunohistochemical studies (28) revealed widespread distribution of the CB_1 receptor in the mouse brain, including basal ganglia, signifying an important role in the CNS. Cannabinoids and the CB_1 receptor exert neuroprotective effects in response to neurotoxic stimuli. Arvanil, a synthetic AEA analog, acts against ouabain-induced excitotoxicity via CB_1 receptor activation and prevents neuronal cell death in vivo (29). HU210 displays neuroprotective activity against excitotoxicity in a multiple sclerosis model (30). WIN55,212-2 protects against ventral tegmental area DA neuronal death under ischemic conditions in vivo and in vitro (31). The actions of these two compounds are inhibited by CB_1 receptor antagonists, such as SR14716A, indicative of CB_1 receptor-mediated neuroprotection. Interestingly, acute injection of rimonabant (SR14716A) has been shown to rescue DA neurons and improve motor deficits in a 6-hydroxydopmaine (6-OHDA) model of PD (32, 33), supporting CB_1 receptor-mediated neurotoxicity.

Notably, AEA is increased in the cerebrospinal fluid of PD patients (34) and animal models of PD produced by administration of 6-OHDA (35). In an MPTP-treated macaque model, increases in AEA and 2-arachidonoylglycerol compensate for dopamine depletion (36). Plant-derived cannabinoids, such as δ-9-tetrahydrocannabinol and cannabidol, protect nigrostriatal DA neurons from 6-OHDA neurotoxicity in vivo in a CB_1 receptor-independent manner (37). In the current study, we examined whether activation of the CB_1 receptor contributes to neuroprotection of nigrostriatal DA neurons against microglial activation-derived oxidative stress in the MPTP mouse model of PD.

Materials and Methods

Material

Materials were purchased from the following companies: AM251, HU210, and WIN55,212-2 (Tocris). SR14716A was prepared by following the previously reported method (38). HU210, WIN55,212-2, AM251, and SR14716A were dissolved in DMSO and then diluted with sterile PBS (1:10 solution of DMSO/PBS). The final concentration of all vehicles for treatment on animals was 0.1% DMSO, and there was no neurotoxicity, compared with vehicle-untreated controls.

Animals and drugs treatment

All experiments were performed in accordance with the approved animal protocols and guidelines established by Kyung Hee University [KHUASP (SE)-10-030]. Eight-week-old male C57BL6 mice (23–25 g; Charles River Breeding Laboratory) were used. For MPTP intoxication, mice received four i.p. injections of MPTP (20 mg/kg, free base; Sigma-Aldrich) dissolved in saline at 2-h intervals. The nonselective cannabinoid receptor agonists WIN55212-2 and HU210 received various doses of the drug (0.1 μg/kg body weight once a day, 1 μg/kg body weight once a day, 10 μg/kg once a day, 20 μg/kg twice a day, and 50 μg/kg/once a day) into the peritoneum for 2 d before the MPTP injections and the specified time periods commencing 12 h after the last MPTP injection for 8 d (Supplemental Fig. 1). The CB_1 receptor antagonists AM251 and SR14716A received the drug (20 μg /kg once a day) into the peritoneum for 30 min before the CB_1 receptor agonist injections. Control mice were injected with CB_1 receptor agonists and antagonists alone or the vehicle. WIN55212-2, HU210, AM251, and SR14716A were prepared by following the previously reported method (39).

Tissue preparation and Immunostaining

Animals were transcardially perfused with saline solution containing 0.5% sodium nitrate and heparin (10 U/ml) and fixed with 4% paraformaldehyde dissolved in 0.1 M phosphate buffer (PB). Brains were dissected from the skull, postfixed overnight in buffered 4% paraformaldehyde at 4˚C, stored in 30% sucrose solution at 4˚C until they sank, and freeze-sectioned with a sliding microtome into 30-μm-thick coronal sections. All sections were collected in six separate series and processed for immunostaining, as described previously (4, 5). In brief, brain sections were rinsed in PBS and incubated overnight at room temperature (RT) with primary Abs, specifically anti–macrophage Ag complex-1 (MAC-1; 1:200 dilution; Serotec, Oxford, U.K.) for microglia and anti-tyrosine hydroxylase (TH; 1:2000 dilution; Pel-Freez Biologicals, Rogers, AR) for DA neurons. The following day, sections were rinsed with PBS and 0.5% BSA, incubated with the appropriate biotinylated secondary Ab, and processed with an avidin-biotin complex kit (Vectastain ABC kit; Vector Laboratories, Burlingame, CA). Bound antiserum was visualized by treatment with 0.05% diaminobenzidine-HCl and 0.003% hydrogen peroxide in 0.1 M PB. The diaminobenzidine reaction was terminated by rinsing tissues in 0.1 M PB. Labeled tissue sections were mounted on gelatin-coated slides and analyzed under a bright-field microscope (Nikon, Melville, NY). For double-immunofluorescence staining, the sections were incubated in a combination of goat polyclonal Ab to NADPH oxidase subunits mouse anti-$p67^{phox}$ (1:500 dilution; BD Biosciences, San Diego, CA), rabbit anti-$p47^{phox}$ (1:200 dilution; Santa Cruz Biotechnology), or mouse anti-$gp91^{phox}$ (1:500; BD Biosciences), and a rat mAb against MAC-1 (Serotec; 1:200 dilution) overnight at 4˚C. After washing in PBS, sections were treated simultaneously with a mixture of FITC-conjugated rabbit anti-rat IgG (1:200 dilution; Vector Laboratories) and Texas Red-conjugated donkey anti-goat IgG (1:200 dilution; Molecular Probes) for 1 h at RT. Slides were mounted with Vectashield medium (Vector Laboratories) and viewed using an IX71 confocal laser scanning microscope (Olympus Optical, Tokyo, Japan). To determine the localization of different Ags in double-stained samples, images were obtained from the same area and merged using interactive software.

Stereological cell counts

The total number of TH-positive neurons was counted in the various animal groups at 7 d postinjection (MPTP or saline) using the optical fractionator method performed on an Olympus Computer Assisted Stereological Toolbox system version 2.1.4 (Olympus Denmark, Ballerup, Denmark) as previously described (4, 5). Actual counting was performed using a 100× oil objective. The total number of neurons was estimated according to the optical fractionator equation (40). More than 300 points over all sections of each specimen were analyzed.

Densitometric analysis

As previously described (4, 5), the OD of TH-positive fiber in striatum (STR) was examined at ×5 original magnification using the IMAGE PRO PLUS system (Version 4.0; Media Cybernetics, Silver Spring, MD) on a computer attached to a light microscope (Zeiss Axioskop, Oberkochen, Germany) interfaced with a CCD video camera (Kodak Mega Plus model 1.4 I; Kodak, New York, NY). To control variations in background illumination, the average of background density readings from the corpus callosum was subtracted from that of density readings of the STR for each section. For each animal, the average of all sections was calculated separately before data were statistically processed.

Measurement of dopamine levels in the STR

The measurement of dopamine was performed as described previously (4, 5). The samples were analyzed for dopamine, separated with a Waters Symmetry C18 column (5 μm; 150 × 4.6 mm; Waters) at 35˚C, and detected electrochemically using a Waters 2465 detector (Waters). The mobile phase consisted of 75 mM NaH_2PO_4, 1.7 mM 1-octanesulfonic acid, 100 μl/l triethylamine, 25 μM EDTA, 9% acetonitrile, and 2 mM NaCl and adjusted to pH 2.9 with concentrated HCl. The amounts of dopamine were calculated using Waters EMPOWER software (Millipore, Milford, MA). A standard curve was constructed with known amounts of dopamine.

Measurement of MPTP and 1-methyl-4-phenyl-pyridinium levels in the STR

As described previously (5), striatal MPTP and 1-methyl-4-phenyl-pyridinium (MPP^+) levels were measured by liquid chromatography

Downloaded from http://journals.aai.org/jimmunol/article-pdf/187/12/6508/1342902/1102435.pdf by guest on 19 April 2024

electrospray ionization mass spectrometry. Dissected striatal tissues were sonicated and centrifuged at 9000 rpm for 20 min in chilled 0.1 M perchloric acid (400 μl), and 100 μl supernatant was isocratically eluted through a 150 mm × 1.5 mm internal diameter, 4 μm Zorbax Eclipse XDB-C18 column (Agilent Technologies, Palo Alto, CA) maintained at 23°C at a flow rate of 0.2 ml min^{-1} for the separation of MPTP and MPP^+. The retention times of MPTP and MPP^+ were 6.967 and 7.763 min, respectively. All samples were normalized for protein content, as determined spectrophotometrically using the Bio-Rad protein assay kit (Bio-Rad, Hercules, CA).

Rotarod test

To determine forelimb and hindlimb motor coordination and balance, we used an accelerating rotarod (UgoBasile, Comerio, Italy), as previously described (5). To acclimate mice on the rotarod apparatus, animals were given a training session (10 rpm for 20 min), 7 consecutive d before MPTP injection. Animals that stayed on the rod without falling during training were selected and randomly divided into experimental groups. On 7 d from final MPTP injection, mice receiving various treatment regimes were placed on the rotating rod and tested at 20 rpm for 20 min. The latency to fall off the rotarod within this time period was recorded by magnetic trip plates.

In situ detection of O_2^- and O_2^--derived oxidants

Three day after last MPTP injection, 200 μg/μl hydroethidine (Molecular Probes; 1 mg/ml in PBS containing 1% DMSO) was administered i.p. After 15 min, the animals were transcardially perfused, postfixed, and the brains were cut into 30 μm. Hydroethidine histochemistry was performed for in situ visualization of O_2^- and O_2^--derived oxidants, as previously described (5). The oxidized hydroethidine product, ethidium, was examined by confocal microscopy (Olympus).

Western immunoblotting

Brain tissues from animals were dissected and then prepared as described previously (4). Equal amounts of protein (30 μg) were mixed with loading buffer (0.125 M Tris-HCl [pH 6.8], 20% glycerol, 4% SDS, 10% mercaptoethanol, and 0.002% bromophenol blue), boiled for 5 min, and separated by SDS-PAGE. After electrophoresis, proteins were transferred to polyvinylidene difluoride membranes (Millipore, Bedford, MA) using an electrophoretic transfer system (Bio-Rad). Membranes were washed with TBS solution, blocked for 1 h in TBS containing 5% skimmed milk, and incubated overnight at 4°C with one of the following specific primary Abs: goat anti–rac-1 (1:1000; Santa Cruz Biotechnology) and rabbit anti-$p47^{phox}$ (1:1000 dilution; Santa Cruz Biotechnology). After washing, membranes were incubated for 1 h at RT with secondary Abs (1:2000 dilution; Amersham Biosciences, Arlington Heights, IL) and rewashed. Finally, blots were developed with ECL detection reagents (Amersham Biosciences) and reprobed with Abs against actin (1:2000 dilution; Santa Cruz Biotechnology). To determine the relative degree of purification, the membrane fraction was subjected to immunoblotting for the marker, calnexin, using a rabbit polyclonal Ab (1:1000 dilution; Stressgen, Victoria, BC, Canada). For semiquantitative analyses, band densities on immunoblots were measured using the Computer Imaging Device and accompanying software (Fujifilm).

Detection for protein carbonylation

As previously described (5), the extent of protein oxidation was assessed by measuring protein carbonyl levels with an OxyBlot protein oxidation detection kit (Chemicon, Temecula, CA) according to the protocol of the manufacturer. Protein samples were prepared from mice SN tissues harvested 3 d after injection with MPTP in the absence or presence of CB_1 agonists and/or antagonists. Subsequently, protein samples (15 μg) were mixed in a microcentrifuge tube with 5 μl 12% SDS and 10 μl 1× 2,4-dinitrophenylhydrazine (DNPH) solution. Tubes were incubated at RT for 15 min and then mixed with 7.5 μl neutralization solution. Next, the samples were mixed in equal volumes of SDS sample buffer and separated by SDS-PAGE. After electrophoresis, proteins were transferred to polyvinylidene difluoride membranes (Millipore). The membranes were then blocked for 1 h at RT in TBS containing 0.1% Tween 20 and 1% BSA. Membranes were incubated overnight at RT with the anti-DNPH Ab (1:150) and then incubated at RT for 1 h with secondary Abs (1:300). Blots were developed using ECL reagents (Amersham Biosciences). Proteins that underwent oxidative modification (i.e., carbonyl group formation) were identified as a band in the samples derivatized with DNPH. The OD of the bands was measured using the Computer Imaging Device and accompanying software (Fujifilm). Levels of protein carbonyls were quantified and expressed as the fold increase versus untreated controls.

Real-time PCR

Animals treated with or without nonselective agonists and/or CB_1 receptor antagonist were decapitated 1 d after injection of MPTP, and the bilateral SN regions were immediately isolated. Total RNA was prepared with RNAzol B (Tel-Test, Friendwood, TX), and reverse transcription was carried out using Superscript II reverse transcriptase (Life Technologies, Rockville, MD) according to the manufacturer's instructions. The primer sequences used in this study were as follows: 5′-TGATGTTCCCATTAGACAGC-3′ (forward) and 5′-GAGGTGCTGATGTACCAGTT-3′ (reverse) for IL-1β; 5′-GCGACGTGGAACTGGCAGAAGAG-3′ (forward) and 5′-TGAGAGGGAGGCCATTTGGGAAC-3′ (reverse) for TNF-α; and 5′-TCCCTCAAGATTGTCAGCAA-3′ (forward) and 5′-AGA TCCACAACGGATACATT-3′ (reverse) for GAPDH. Real-time PCRs were performed in a reaction volume of 20 μl including 1 μl reverse transcription product as a template, 10 μl SYBR Green PCR master mix (Applied Biosystems, Warrington, U.K.), and 20 pmol each primer described above. The PCR amplifications were performed with 40 cycles of 95°C for 30 s and 60°C for 60 s using an ABI 7500 (Applied Biosystems). Average threshold cycle (Ct) values of IL-1β and TNF-α from triplicate PCR reactions were normalized from average Ct values of GAPDH. To express the relative amount of IL-1β and TNF-α, the ΔΔCt value was calculated by subtracting the ΔCt value of control group from the ΔCt value of each group. The ratios of expression levels of IL-1β and TNF-α were calculated as $2^{-(\text{mean}\Delta\Delta Ct)}$.

Measurement of proinflammatory cytokines

At 3 d from final MPTP treatment, mice treated with or without nonselective cannabinoid receptor agonists and/or CB_1 receptor antagonists were sacrificed, and then SN tissues were isolated. The amount of IL-1β and TNF-α from SN was measured with sandwich ELISA techniques. Tissues were prepared for ELISA as described (4, 5). Equal amounts of protein (100 μg) from each sample were placed in ELISA kit strips coated with the appropriate Ab. Sandwich ELISA was then performed according to the manufacturer's instructions (BioSource International, Camarillo, CA). The detection limits of IL-1β and TNF-α were 5 pg/ml and 25 pg/ml, respectively.

Neuron-enriched mesencephalic cultures and drug treatment

SD rat ventral mesencephalon tissues were isolated from embryonic day 14 fetal brain and dissected (5). Tissues were cut into small segments and incubated in Ca^{2+}-, Mg^{2+}-free HBSS for 10 min at 37°C. Cultures were replaced with 0.01% trypsin solution in Ca^{2+}-, Mg^{2+}-free HBSS, incubated for an additional 9 min, rinsed twice in DMEM (Life Technologies), supplemented with 10% FBS, 6 mg/ml glucose, 204 μg/ml L-glutamine, and 100 U/ml penicillin/streptomycin, and mechanically triturated. Dissociated cells were plated on 12-mm round aclar plastic coverslips (1.0×10^5 cells/coverslip) precoated with 0.1 mg/ml poly-D-lysine and 4 μg/ml laminin and housed in 24-well culture plates. Cells were maintained in a humidified incubator at 37°C, 5% CO_2, for 24 h. The media of 2-d-old in vitro cultures (days in vitro [DIV] 2) incubated in the absence of serum were replaced with chemically defined serum-free medium composed of Ham's nutrient mixture (F12-DMEM) and supplemented with 1% insulin, transferrin, selenium, glucose, L-glutamine, and penicillin/streptomycin. At 4 DIV, cultures were transferred to defined serum-free medium without insulin, transferrin, selenium, treated MPP^+ for 48 h, and processed for further experiments.

Cocultures of mesencephalic neurons and microglia

Mesencephalic microglia cultures were prepared from the ventral mesencephalons of embryonic day 14 SD rat brain as previously described (5). Tissues were triturated and plated in 75-cm^2 T-flasks precoated with poly-D-lysine at a density of 1×10^7 cells/flask, and then maintained in DMEM supplemented with 10% FBS. After 2 to 3 wk, microglia were detached from the flasks applied to a nylon mesh to remove astrocytes. At 3 DIV, neuron-enriched mesencephalic cultures plated on 12-mm round aclar plastic coverslips (1×10^5 cells/coverslip) housed in 24-well plates were supplemented with 5×10^4 mesencephalic microglia/well. After 1 h, the culture medium was replaced with neuronal culture medium (DMEM [Life Technologies] containing 2% FBS); 24 h later, the cocultures were treated with MPP^+ for 48 h and processed for further experiments.

Statistical analysis

All values are expressed as mean ± SEM. Statistical significance was assessed by two-way ANOVA using Instat 3.05 (GraphPad), followed by Student–Newman–Keuls analyses.

Downloaded from http://journals.aai.org/jimmunol/article-pdf/187/12/6508/1342902/1102435.pdf by guest on 19 April 2024

Results

WIN55,212-2 and HU210 protect nigrostriatal DA neurons from the MPTP neurotoxicity in vivo

After 7 d from last MPTP injection, the mice were sacrificed for immunohistochemical assessments. The brain tissues were immunostained with a TH Ab for detecting DA neurons (Figs. 1*A–L*, 2*A–F*). TH immunostaining revealed that four injections of MPTP led to damage in SN (Fig. 1*C*, 1*D*) and STR (Fig. 2*B*) compared with saline-treated control groups (Figs. 1*A*, 1*B*, 2*A*). DA neuronal cells were quantified as the stereological count of TH-positive cells in the SN and OD of TH-positive fibers in the STR. The quantitative data confirmed that MPTP induces 71% ($p < 0.001$) DA neuronal death in SN and 77% loss in TH-positive fibers in STR ($p < 0.001$), respectively, compared with PBS-treated mice as controls. By contrast, mice treated with nonselective cannabinoid receptor agonists WIN55,212-2 and HU210 led to a dramatic increase of TH-positive neurons in SN (Fig. 1*E–H*) and fibers in STR (Fig. 2*C*, 2*D*). Treatment of 0.1 μg/kg and 1 μg/kg WIN55,212-2 and HU210 had no effects (Supplemental Table I), whereas 10 μg/kg WIN55,212-2 and HU210 produced 59% ($p < 0.001$) and 54% ($p < 0.001$) increase in TH-positive cells numbers in SN, respectively, compared with MPTP-treated mice (Fig. 1*M*). Moreover, WIN55,212-2 and Hu210 led to 66% ($p < 0.001$) and 56% ($p < 0.001$) increase in TH-positive nerve terminals in STR (Fig. 2*G*).

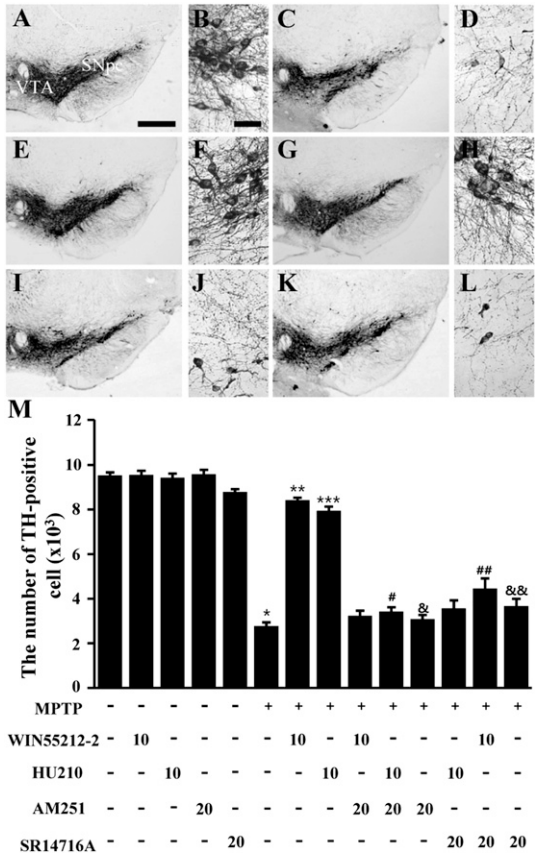

FIGURE 1. Activation of CB_1 receptor attenuates MPTP-induced neurotoxicity in the SN of mouse brain. Animals receiving PBS as a control (*A*, *B*) or MPTP (*C*, *D*), MPTP and WIN55,212-2 (*E*, *F*), MPTP and HU210 (*G*, *H*), MPTP, WIN55,212-2, and SR14716A (*I*, *J*), or MPTP, HU-210, and SR14716A (*K*, *L*) were sacrificed 7 d after last MPTP injection. Brain tissues were cut, and SN tissues were immunostained with TH Ab for DA neurons. *B*, *D*, *F*, *H*, *J*, *L* are higher magnifications of *A*, *C*, *E*, *G*, *I*, *K*, respectively. Scale bars, *A*, *C*, *E*, *G*, *I*, *K*, 300 μm; *B*, *D*, *F*, *H*, *J*, *L*, 50 μm. *M*, Numbers of TH-positive neurons in the SN were counted. Five to 11 animals were used for each experimental group. $^{*}p < 0.001$, significantly different from controls; $^{**}p < 0.001$, $^{***}p < 0.001$, significantly different from MPTP; $^{\#}p < 0.001$, $^{\&}p < 0.001$, significantly different from MPTP and WIN55,212-2, MPTP and Hu210; $^{\#\#}p < 0.001$, $^{\&\&}p < 0.001$, significantly different from MPTP and WIN55,212-2, MPTP, and Hu210 (ANOVA and Student–Neuman–Keuls analysis). SNpc, substantia nigra pars compacta; VTA, ventral tegmental area.

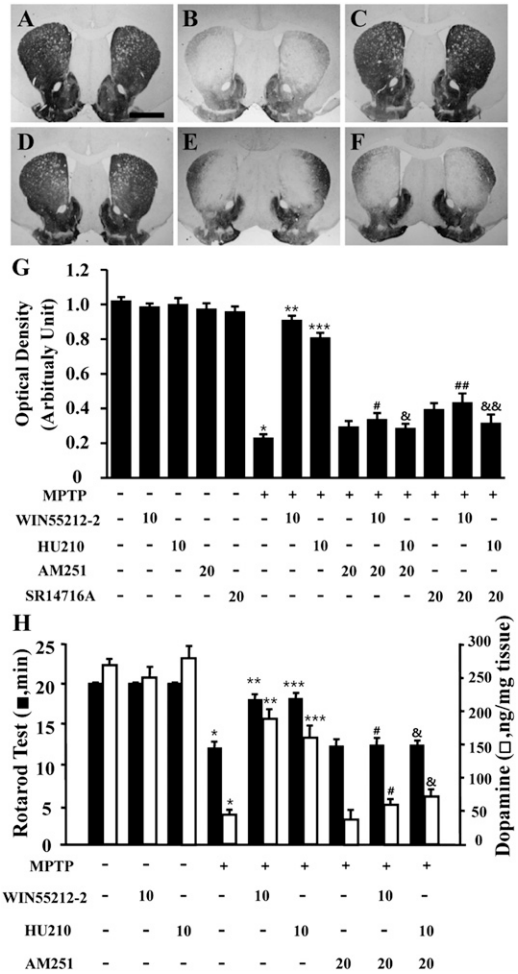

FIGURE 2. Activation of CB_1 receptor protects MPTP-induced neurotoxicity in the STR in vivo. The striatal tissues obtained from the same animals as used in Fig. 1 were immunostained with TH Ab for DA fibers. PBS as a control (*A*), MPTP (*B*), MPTP and WIN55,212-2 (*C*), MPTP and HU210 (*D*), MPTP, WIN55,212-2, and SR14716A (*E*), and MPTP, HU-210, and SR14716A (*F*). Scale bar, *A–F*, 500 μm. *G*, The OD of TH-positive fibers in the STR. *H*, Nonselective cannabinoid receptor agonists increase striatal dopamine level and produce motor recovery. Rotarod test was performed 7 d after last MPTP injection, and then striata were prepared for HPLC analysis. Five to seven animals were used for each experimental group. $^{*}p < 0.001$, significantly different from control; $^{**}p < 0.001$,$^{***}p < 0.001$, significantly different from MPTP; $^{\#}p < 0.001$, $^{\&}p < 0.001$, significantly different from MPTP and WIN55,212-2, MPTP, and Hu210; $^{\#\#}p < 0.001$, $^{\&\&}p < 0.001$, significantly different from MPTP and WIN55,212-2, MPTP, and Hu210 (ANOVA and Student–Neuman–Keuls analysis).

To ascertain whether this neuroprotective action was mediated by activation of CB_1 receptor in vivo, we examined the effect of CB_1 receptor antagonists AM251 and SR14716A in MPTP mice. AM251 (20 μg/kg) decreased TH-positive cells numbers in the SN by 47% ($p < 0.001$) and 55% ($p < 0.001$) (Fig. 1*M*) and TH-positive fibers in the STR by 47% ($p < 0.001$) and 55% ($p < 0.001$) (Fig. 2*G*), respectively, compared with MPTP plus

Downloaded from http://journals.aai.org/jimmunol/article-pdf/187/12/6508/1342902/1102435.pdf by guest on 19 April 2024

WIN55,212-2–treated or MPTP plus HU210-treated mice. Additional experiments were performed to corroborate CB_1 receptor-mediated neuroprotection by using another CB_1 receptor antagonist, SR14716A. Consistent with AM251, pretreatment of 20 μg/kg SR14716A attenuated the survival of TH-positive neurons in the SN treated with MPTP plus WIN55,212-2 (36%; $p < 0.001$) or MPTP plus HU210 (49%, $p < 0.001$) (Fig. 1*M*). SR14716A also decreased the protective effect on TH-positive fiber in STR treated with MPTP plus WIN55,212-2 (32%; $p < 0.001$) or MPTP plus HU210 (44%; $p < 0.001$) (Fig. 2*G*), further indicative of CB_1 receptor-mediated neuroprotection. As controls, AM251 or SR14716A alone had no effects (Figs. 1*M*, 2*G*).

WIN55,212-2 and HU210 increase striatal dopamine levels and improves motor behavior in MPTP mice

We next determined whether WIN55,212-2 and HU210 recover MPTP-induced motor deficits by testing rotarod performance (4). MPTP treatment decreased sustained rotarod time to 11.65 ± 0.53 min compared with that of PBS treatment (Fig. 2*H*; $p < 0.001$). By contrast, WIN55,212-2 and HU210 partially improve behavioral dysfunction, which increased the latency to falling to 18.52 ± 0.29 min (Fig. 2*H*; $p < 0.001$) and 18.26 ± 0.41 min (Fig. 2*H*; $p < 0.001$), respectively.

After rotarod performance test, the mice were sacrificed for measuring striatal dopamine levels using HPLC analysis. In parallel with motor deficits, quantification of striatal dopamine levels revealed that MPTP induces 79% reduction of dopamine levels (Fig. 2*H*; $p < 0.001$). By contrast, WIN55,212-2 and HU210 increased striatal dopamine levels in MPTP mice by 48% (Fig. 2*H*; $p < 0.001$) and 44% (Fig. 2*H*, $p < 0.001$). These behavioral and biochemical effects of WIN55,212-2 and HU210 were significantly reversed by AM251 (Fig. 2*H*). As controls, WIN55,212-2, HU210, and AM251 alone had no effects on behavior and dopamine levels.

WIN55,212-2 and HU210 do not alter the metabolism of MPTP to MPP^+

MPTP neurotoxicity correlates linearly to the striatal levels of MPP^+, an active toxic metabolite of MPTP converted by monoamine oxidase-B, in mouse brain (41). To determine whether the observed neuroprotection of WIN55,212-2 and HU210 was attributable to alteration of MPTP conversion to MPP^+, we measured the striatal content of MPTP and MPP^+ at 2 h after the last injection of MPTP in the presence or absence of WIN55,212-2 and HU210 (Table I). The reason we chose 2 h after the last injection of MPTP is because striatal levels of MPP^+ were peaked at this time point (5). The present results showed that MPP^+ levels in STR did not differ between MPTP-injected mice in the presence or absence of WIN55,212-2 and HU210, although WIN55,212-2 was known to affect the DA transporter (42).

Table I. The effects of nonselective cannabinoid receptor agonists on MPTP and MPP^+ levels (μg/mg protein) in the striata of C57 BL/6 mice

	Control	MPTP	MPTP + WIN55,212-2	MPTP + HU210
MPTP	0	2.5 ± 0.9	2.6 ± 1.1	2.7 ± 1.2
MPP^+	0	3.4 ± 0.2	3.5 ± 0.3	3.6 ± 0.6

For nonselective cannabinoid receptor agonist treatment, mice received a single injection/day of WIN55,212-2 and HU210 (10 μg/kg body weight) into the peritoneum for 3 d, beginning at 30 min before first MPTP injection. After pretreatment, mice received four i.p. injections of MPTP (20 mg/kg body weight) at 2-h intervals. Striatal tissues were removed at 2 h after the last MPTP injection, and MPTP and MPP^+ levels were measured by liquid chromatography electrospray ionization mass spectrometry. Note that there are no changes of striatal MPP^+ levels in the absence and presence of CB agonists.

WIN55,212-2 and HU210 inhibit MPTP-induced microglial activation and ROS production

To determine whether survival of DA neurons by CB_1 receptor activation is due to suppress the microglial activation in the SN in vivo, we performed the immunostaining with MAC-1 and ED-1 Ab to detect microglial activation. In PBS-treated control mice, only a few faintly immunorecative microglia with resting morphology (ramification with small cell bodies and thin processes) were observed in the SN (Fig. 3*A*). In MPTP-treated mice, numerous MAC-1–positive activated microglia with larger cell bodies and thick processes were observed in the SN (Fig. 3*D*). By contrast, in MPTP mice treated with WIN55,212-2 (Fig. 3*G*) or HU210 (Fig. 3*J*), MAC-1 immunostaining was similar to those observed in PBS-treated mice. This inhibitory effect was reversed by AM251, a CB_1 receptor antagonist (Fig. 3*M*, 3*P*).

Microglia in the MPTP-treated SN appeared to reach a state similar to that of active phagocytes (Fig. 3*E*), as determined by ED1 immunohistochemical staining, which labels phagocytic microglia, in particular the presence of injured cells or debris (4). Consistent with MAC-1 immunostaining results, few ED1-positive cells were observed in MPTP mice treated with WIN55,212-2 (Fig. 3*H*) and HU210 (Fig. 3*K*). This inhibitory effect was reversed by AM251, CB_1 receptor antagonist (Fig. 3*N*, 3*Q*). CB_1

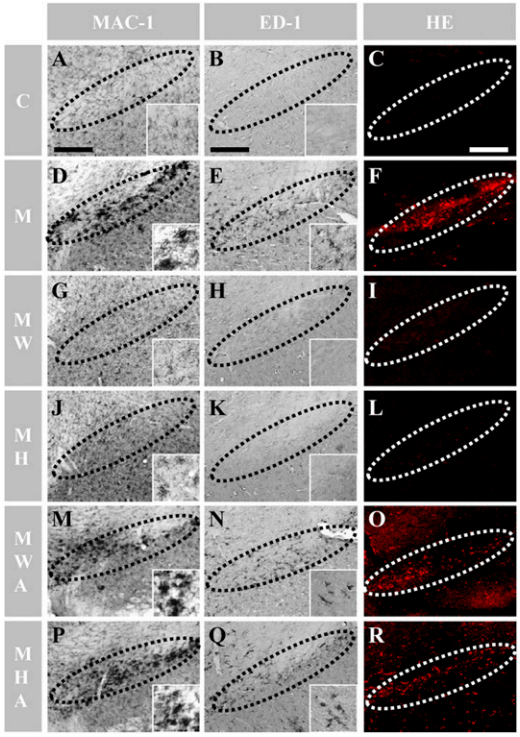

FIGURE 3. Activation of CB_1 receptor inhibits microglial activation and oxidants production in the SN in vivo. Animals receiving vehicle as a control (*A–C*), or MPTP (*D–F*), MPTP and WIN55,212-2 (*G–I*), MPTP and HU-210 (*J–L*), MPTP, WIN55,212-2, and AM251 (*M–O*), or MPTP, HU210, and AM251 (*P–R*) were sacrificed 3 d after last MPTP injection. SN tissues were prepared for MAC-1 (*A*, *D*, *G*, *J*, *M*, *P*) and ED-1 (*B*, *E*, *H*, *K*, *N*, *Q*) immunostaining to detect microglia or for hydroethidine (HE) histochemistry to detect the oxidants production (*C*, *F*, *I*, *L*, *O*, *R*). Five to seven animals were used for each experimental group. *Insets* show higher magnifications of *A*, *B*, *D*, *E*, *G*, *H*, *J*, *K*, *M*, *N*, *P*, *Q*, respectively. Dotted lines indicate SNpc. Scale bars, *A*, *B*, *D*, *E*, *G*, *H*, *J*, *K*, *M*, *N*, *P*, *Q*, 200 μm; *C*, *F*, *I*, *L*, *O*, *R*, 150 μm. C, control; M, MPTP; MH, MPTP and HU210; MHA, MPTP, HU210, and AM251; MW, MPTP and WIN-55,212-2; MWA, MPTP, WIN-55,212-2, and AM251.

Downloaded from http://journals.aai.org/jimmunol/article-pdf/187/12/6508/1342902/1102435.pdf by guest on 19 April 2024

receptor agonists and antagonists alone had no effect on microglial activation (data not shown).

In MPTP-treated mice, activated microglia produce O_2^- and O_2^--derived oxidants that contributed to DA neuronal death in the SN via oxidative stress (4, 7). Accordingly, we examined whether WIN55,212-2 and HU210 rescued nigral DA neurons by inhibiting MPTP-induced oxidant production. MPTP-treated mice showed a significant increase in the fluorescent products of oxidized hydroethidine (i.e., ethidium accumulation) in the SN at 3 d from MPTP injection (Fig. 3*F*) compared with PBS-treated mice (Fig. 3*C*). Treatment with WIN55,212-2 (Fig. 3*I*) and HU210 (Fig. 3*L*) diminished ethidium accumulation in MPTP mice. In contrast, AM251 significantly increased the reduced oxidants level in the SN treated with MPTP plus WIN55,212-2 (Fig. 3*O*) and MPTP plus HU210 (Fig. 3*R*).

WIN55,212-2 inhibits MPTP-induced activation of microglial NADPH oxidase in the SN

NADPH oxidase is composed of cytosolic component, including $p47^{phox}$, $p67^{phox}$, Rac-1, and a membrane component, such as $gp91^{phox}$ (43, 44). This enzyme produces O_2^- and O_2^--derived oxidants through translocation of its subunits from the cytosol to plasma membrane in activated glial cells, which eventually contributes to DA neuronal death in MPTP-treated mice (4). To examine whether WIN55,212-2 affects the activity of NADPH oxidase in the SN, we accomplished the Western blot after separating into membrane and cytosolic components. At 3 d after the final MPTP injection, levels of cytosolic NADPH oxidase subunits ($p47^{phox}$ and Rac-1) were significantly increased in the membrane fraction (Fig. 4*A*, 4*B*; $p < 0.01$), indicative of translocation and activation of the complex. MPTP-induced translocation of $p47^{phox}$ (Fig. 4*A*, 4*B*; $p < 0.01$) and Rac-1 (Fig. 4*A*, 4*B*; $p < 0.01$) were dramatically decreased in SN treated with WIN55,212-2. This effect was reversed by AM251, a CB_1 receptor antagonist. WIN55,212-2 alone had no effects. Additional double-immunofluorescence staining demonstrated in vivo that, in MPTP-treated SN, the $p47^{phox}$-, $p67^{phox}$-, and $gp91^{phox}$-positive cells (Fig. 4*C–E*, red) were localized within MAC-1–positive microglia (Fig. 4*C–E*, green), but not astrocytes or neurons (data not shown).

WIN55,212-2 and HU210 attenuate MPTP-induced oxidative damages

ROS derived from NADPH oxidase mediates MPTP neurotoxicity through oxidative damage on cellular components such as nucleic acids, proteins, and lipids (3). The levels of 8-hydroxy-2-deoxyguanosine (8-OHdG), a marker of oxidative nucleic acid damage, are increased in cerebrospinal fluid of PD patients (45) and MPTP mice (4, 5). To determine the effects of WIN55,212-2 and HU210 on MPTP-induced oxidative damage in nucleic acids, we immunostained for 8-OHdG. Substantial increases in 8-OHdG content were evident in the SN 3 d after the final MPTP injection (Fig. 5*C*, 5*D*) compared with the SN of PBS-treated controls (Fig. 5*A*, 5*B*). This MPTP-induced increase in 8-OHdG levels was significantly abrogated in the SN treated with WIN55,212-2 (Fig. 5*E*, 5*F*) and HU210 (Fig. 5*G*, 5*H*). This effect was reversed by AM251 (Fig. 5*I–L*). As controls, WIN55,212-2, HU210, and AM251 alone had no effects (data not shown).

Oxidative damage to proteins is significantly increased in the SN of PD patients (46, 47) and MPTP mice (5). MPTP-induced protein oxidative damage was assessed by measuring protein carbonylation in the SN. Western blot analysis revealed that the levels of protein carbonyls were significantly increased in MPTP-treated SN compared with controls (Fig. 5*M*, 5*N*; $p < 0.01$). By contrast, treatment with HU210 reduced MPTP-induced increase

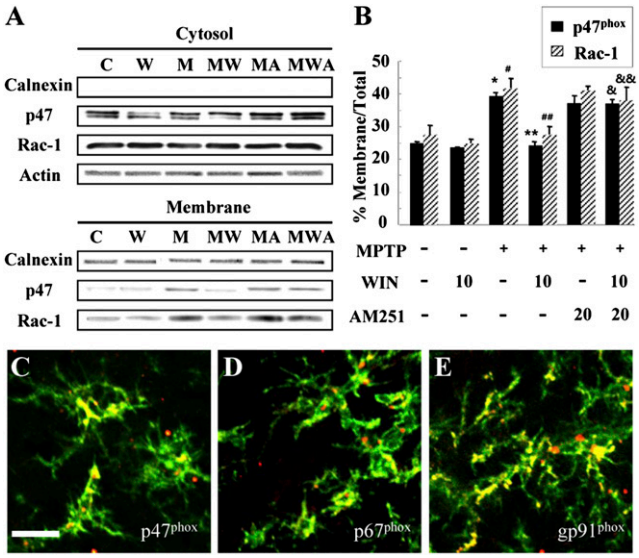

FIGURE 4. Activation of CB_1 receptor inhibits MPTP-induced NADPH oxidase activation in the SN in vivo. *A*, Tissue lysates from the SN were prepared 3 d after last MPTP injection or vehicle in the absence or presence of WIN55,212-2 and/or AM251, CB_1 receptor antagonist. Fractionated proteins were analyzed by SDS-PAGE and subjected to immunoblotting with anti-$p47^{phox}$ or anti–Rac-1 Ab. The membrane protein calnexin was used to normalize the data. Translocation of cytosolic subunits ($p47^{phox}$ and Rac-1) from the cytosol to the plasma membrane after MPTP injection, indicating activation of NADPH oxidase in the SN; this translocation was inhibited by WIN55,212-2, CB_1 receptor agonist. *B*, The histogram shows quantitation of $p47^{phox}$ and Rac-1 levels expressed as the ratio of membrane fraction to total. The results represent the means ± SEM of four to five separate experiments. Localization of $p47^{phox}$, $p67^{phox}$, and $gp91^{phox}$ within the activated microglia in the SN treated with MPTP. The SN tissues were prepared 3 d after last MPTP injection and immunostained with Ab to MAC-1 (green) and $p47^{phox}$ (red) (*C*), $p67^{phox}$ (red) (*D*), or $gp91^{phox}$ (red) (*E*). Scale bar, 50 μm. $^*p < 0.01$ and $^{\#}p < 0.01$, significantly different from control; $^{**}p < 0.01$ and $^{\#\#}p < 0.01$, significantly different from MPTP; $^{\&}p < 0.01$ and $^{\&\&}p < 0.01$, significantly different from MPTP and WIN55,212-2 (ANOVA and Student–Neuman–Keuls analysis).

in the levels of protein carbonyls (Fig. 5*M*, 5*N*; $p < 0.01$). This effect was reversed by AM251 (Fig. 5*M*, 5*N*; $p < 0.05$).

WIN55,212-2 and HU210 inhibit MPTP-induced expression of IL-1β and TNF-α

Several lines of evidence have demonstrated that mice expressing a dominant-negative inhibitor of IL-1β–converting enzyme or those deficient in TNF-α are resistant to MPTP-induced neurotoxicity (10, 11). Thus, we examined whether WIN55,212-2 and HU210 affect MPTP-induced expression of IL-1β and TNF-α, resulting in DA neuronal survival. Real-time PCR analysis showed that WIN55,212-2 and HU210 dramatically inhibited MPTP-induced mRNA expression of IL-1β and TNF-α at 1 d after the last MPTP injection (Fig. 6*A*). As expected, these inhibitory effects were almost completely reversed by AM251.

To confirm that these changes at the mRNA level are reflected in changes at the protein level, we analyzed tissue lysates by ELISA 3 d after the final MPTP injection (Fig. 6*B*). Similar to real-time PCR results, ELISA analyses showed that the levels of IL-1β and TNF-α protein were significantly increased in the SN of MPTP-treated mice compared with the SN of PBS-treated mice (Fig. 6*B*). Treatment with CB_1 receptor agonists inhibited these MPTP-induced increases, reducing expression of IL-1β by 64 and 55% ($p < 0.01$; Fig. 6*B*) and TNF-α by 51 and 38% ($p < 0.01$; Fig.

Downloaded from http://journals.aai.org/jimmunol/article-pdf/187/12/6508/1342902/1102435.pdf by guest on 19 April 2024

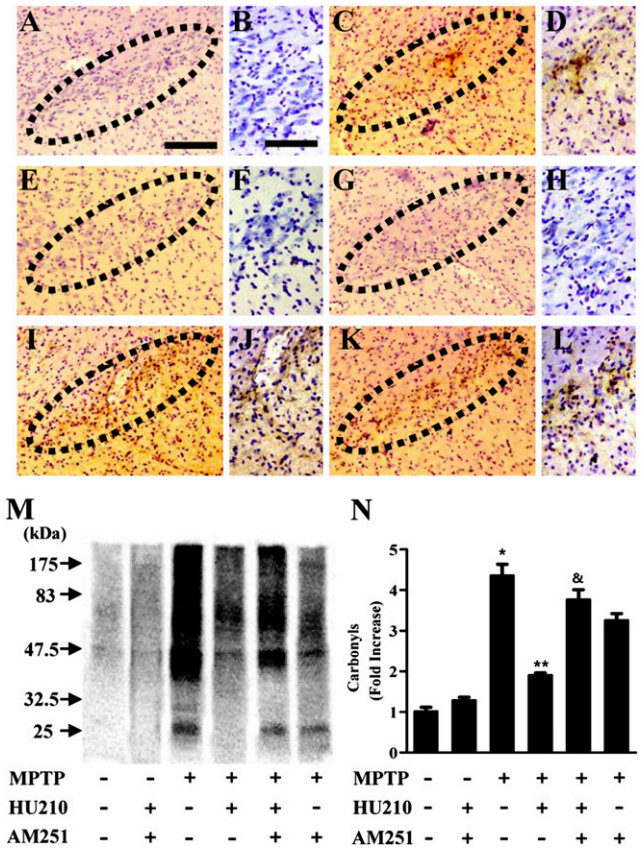

FIGURE 5. Activation of CB_1 receptor prevents oxidative damages on nucleic acids and proteins in MPTP-treated SN in vivo. At 3 d after the final MPTP injection, 8-OHdG immunostaining (brown) and then performed Nissl staining (blue) in mouse SN treated with PBS (*A*, *B*), MPTP (*C*, *D*), or MPTP and WIN55,212-2 (*E*, *F*), MPTP and HU-210 (*G*, *H*), MPTP, WIN55,212-2, and AM251 (*I*, *J*), or MPTP, HU210, and AM251 (*K*, *L*). *B*, *D*, *F*, *H*, *J*, *L* are higher magnifications of *A*, *C*, *E*, *G*, *I*, *K*, respectively. Five to six animals were used for each experimental group. The dotted lines indicate the SNpc. Scale bars, 250 μm. *M* and *N*, Detection for protein oxidation reveals that CB_1 receptor reduces the protein carbonyls in MPTP-treated SN. Samples were analyzed by Western blotting for protein carbonyls as markers of oxidatively modified proteins. *N*, Bars represent the means ± SEM of four to five samples. $^{*}p < 0.01$ compared with control, $^{**}p < 0.01$ compared with MPTP only, $^{\&}p < 0.01$ compared with MPTP and HU210 (ANOVA and Student–Neuman–Keuls analysis).

6*B*) in the SN. However, these anti-inflammatory properties of WIN55,212-2 and HU210 were reduced by AM251. These results further confirm that MPTP-induced expression of proinflammatory cytokines could be regulated by CB_1 receptor activation.

WIN55,212-2 and HU210 protect DA neurons from microglia-derived neurotoxicity

Our results showed that the in vivo neuroprotective effects of nonselective cannabinoid receptor agonists WIN55,212-2 and HU210 are not attributable to reduced metabolism of MPTP to MPP^+ in DA neurons (Table I). However, the possibility remained that WIN55,212-2 and HU210 might promote neuronal survival by preventing MPP^+-induced blockade of mitochondrial respiration in neurons. To test this hypothesis, additional experiments were performed in mesencephalic neurons cultured alone or cocultured with microglia. In microglia-free, neuron-enriched mesencephalic cultures, pretreatment with 0.1–1.0 μM WIN55,212-2 and HU210 (30 min before MPP^+ treatment) had no protective effect (Fig. 7*A–E*, 7*K*), and 3 μM WIN55,212-2 and HU210 alone

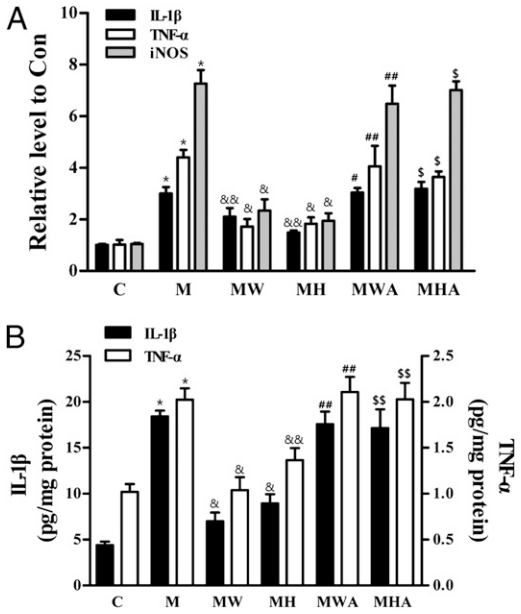

FIGURE 6. Activation of CB_1 receptor attenuates the MPTP-induced inflammation in the SN in vivo. Animals were administered vehicle or MPTP in the absence or presence of WIN-55,212-2 or HU210 and/or AM251, CB_1 receptor antagonist, and sacrificed 1 d later for real-time PCR (*A*) or 3 d later for a sandwich ELISA in the SN (*B*). CB_1 receptor dramatically attenuated MPTP-induced expression of proinflammatory cytokines including IL-1β and TNF-α. Bars represent the means ± SEM of four to five samples. $^{*}p < 0.01$, significantly different from C; $^{\&}p < 0.01$, $^{\&\&}p < 0.05$, significantly different from M; $^{\#}p < 0.01$, $^{\#\#}p < 0.05$, significantly different from MW; $^{\$}p < 0.01$, $^{\$\$}p < 0.05$, significantly different from MH (ANOVA and Student–Neuman–Keuls analysis). C, control; M, MPTP; MH, MPTP and HU210; MHA, MPTP, HU210, and AM251; MW, MPTP and WIN-55,212-2; MWA, MPTP, WIN-55,212-2, and AM251.

was toxic (data not shown). These results carefully suggested that this observed neuroprotection is not due to prevent either MPP^+-induced blockade of mitochondrial respiration in neurons or MPP^+ uptake into DA neurons.

By contrast, in cocultures of mesencephalic neurons and microglia, WIN55,212-2 and HU210 (0.5–1.0 μM) blocked MPP^+-induced death of DA neurons (Fig. 7*F–L*), suggesting that WIN55,212-2 and HU210 act through microglia to mediate its neuroprotective effects. Moreover, pretreatment with AM251 (2 μM), a CB_1 receptor antagonist, reduced the number of TH-positive cells observed with 1 μM WIN55,212-2 (45%; $p < 0.01$; Fig. 7*L*) and 1 μM HU210 (48%; $p < 0.01$; Fig. 7*L*) in MPP^+-treated cocultures of mesencephalic neurons and microglia, indicative of microglia CB_1 receptor involvement (48).

Discussion

Accumulating evidence suggests that the cannabinoid system is a promising pharmacological target for the treatment of PD (49, 50) and levodopa-associated motor complications (51, 52). The CB_1 receptor regulates motor behavior in the basal ganglia via mediating both excitatory and inhibitory inputs to the SN reticulate and globus pallidus (53) as well as short- and long-term synaptic plasticity through suppressing the release of neurotransmitters, such as glutamate and GABA (54, 55). Additionally, cannabinoids modulate inflammatory responses by regulating microglial function through both receptor-dependent and -independent mechanisms (39, 56–58).

Microglia, resident immunocompetent and phagocytic cells in the CNS, play a critical role in innate defense (59). These intrinsic

Downloaded from http://journals.aai.org/jimmunol/article-pdf/187/12/6508/1342902/1102435.pdf by guest on 19 April 2024

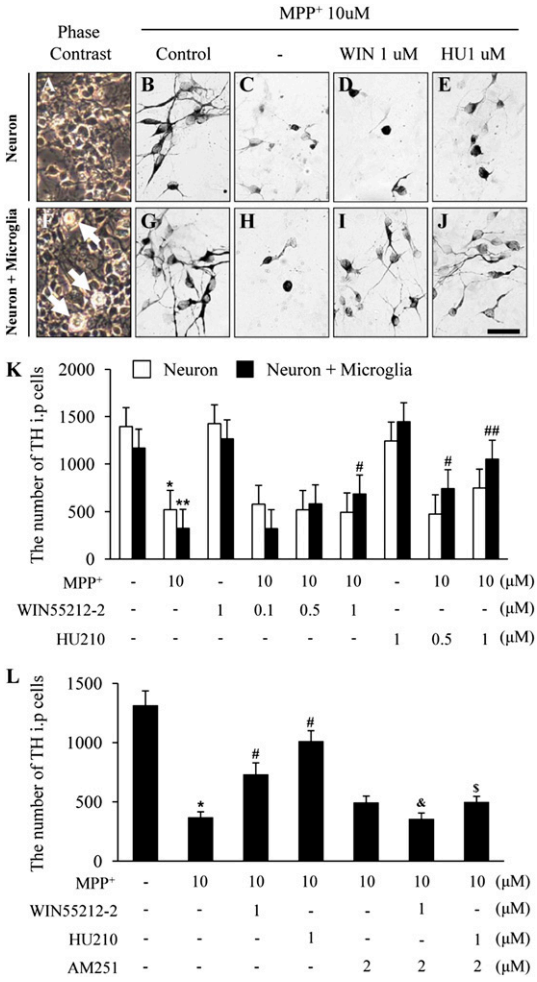

FIGURE 7. Effects of cannabinoids on MPP^+-induced neurotoxicity in mesencephalic cultures. *A* and *F* are phase-contrast optics of *B* and *G*, respectively. Arrows indicate presence of microglia. TH-positive neurons in neuron-enriched mesencephalic cultures treated with vehicle as a control (*B*) and 10 μM MPP^+ for 48 h in the absence (*C*) or presence (*D*) of WIN55,212-2 (0.1–1 μM) and HU210 (0.1–1 μM) (*E*) pretreatment for 30 min. Note that following either MPP^+ or MPP^+ plus WIN55,212-2/HU210, several of the remaining TH-positive neurons displayed short processes and rounded and shrunken cell bodies compared with the vehicle-treated control. These results clearly indicate that WIN55,212-2 and HU210 have no effect against MPP^+-induced neurotoxicity in microglia-free neuron-enriched mesencephalic cultures. TH-positive neurons in cocultures of mesencephalic neurons and microglia treated with vehicle as a control (*G*) and 10 μM MPP^+ for 48 h in the absence (*H*) or presence of WIN55,212-2 (1 μM) (*I*) and HU210 (0.1–1 μM) (*J*) pretreatment for 30 min. Similar to those observed in neuron-enriched cultures (*B–E*), following MPP^+ treatment, many of the remaining TH-positive neurons had short processes and rounded and shrunken cell bodies compared with vehicle-treated control. By contrast, following WIN55,212-2 and HU210 treatment, TH-positive neurons had long and branched neuritic processes, indicating protective effect of WIN55,212-2 and HU210 against MPP^+ neurotoxicity in cocultures. Scale bar, *A–J*, 50 μM. *K*, TH-positive neurons were counted. *L*, Number of TH-positive neurons in cocultures of mesencephalic neurons and microglia treated with MPP^+ in either the absence or presence of WIN55,212-2 or HU210 and CB_1 receptor antagonist. Cultures were pretreated with 2 μM AM251 for 30 min before treatment with 1 μM WIN55,212-2 or HU210 for 48 h. All values are expressed as means ± SEM of triplicate cultures from three separate plates. $^*p < 0.001$, $^{**}p < 0.001$, compared with each control values; $^{\#}p < 0.01$, compared with MPP^+ only-treated cocultures; $^{\#\#}p < 0.05$, compared with MPP^+ only-treated cocultures; $^{\&}p < 0.01$, compared with MPP^+- and WIN55,212-2–treated cocultures; $^{\$}p < 0.01$, compared with MPP^+- and HU210-treated cocultures (ANOVA and Student–Neuman–Keuls analysis).

immune cells perform neuron-protective and -supportive functions in the normal CNS. Under neuropathological conditions, microglia are rapidly activated in response to neuronal damage and produce various potentially neurotoxic compounds, including ROS/reactive nitrogen species and/or proinflammatory cytokines (60).

One such pathogenic condition is PD, in which oxidative damage may account for the degeneration of DA neurons in the SN of PD brain (61, 62). ROS, such as O_2^- and O_2^--derived oxidants, may induce oxidative stress in DA neurons and induce and/or exacerbate MPTP neurotoxicity (63). Numerous studies have shown evidence of oxidative stress in PD patients and MPTP-treated mice, including high levels of oxidative nucleic acid damage (64, 65) and protein oxidation (5, 46). The ROS inducing these molecular modifications are generated by microglial NADPH oxidase and play an important role in the development of oxidative stress in the MPTP model of PD (66). Several studies (7, 67), including our recent investigations (4, 5), have implicated the activation of microglial NADPH oxidase in DA neuron degeneration in SN of MPTP-treated mice. The present study further showed that MPTP induces activation of NADPH oxidase, confirmed by membrane translocation of $p47^{phox}$ and Rac-1, the cytosolic components of NADPH oxidase, resulting in increased ROS and oxidative damage to nucleic acids and proteins in the SN, as assessed using hydroethidine staining, 8-OHdG immunostaining, and Western blot analysis (to ascertain the levels of protein carbonylation), respectively. WIN55,212-2 and HU210 inhibited microglial NADPH oxidase activation and reduced ROS production and nucleic acid and protein oxidation, leading to improved survival of nigrostriatal DA neurons, which was reversed by CB_1 receptor antagonists. These data support the hypothesis that CB_1 receptor-mediated neuroprotective effects are associated with an ability to inhibit microglial NADPH oxidase-derived ROS production and oxidative damage in DA neurons.

In addition to ROS, microglia-derived proinflammatory cytokines may be involved in nigrostriatal DA neuronal death. Several lines of evidence highlight the presence of activated glial cells expressing the proinflammatory cytokines IL-1β and TNF-α in the SN of PD patients (68) and MPTP-treated mice (69). IL-1β and TNF-α originating from activated glial cells may trigger intracellular death-related signaling pathways in the MPTP model of PD (70). This is comparable to our recent finding that activated microglia-derived IL-1β and TNF-α participated in DA neuronal death in an MPTP mouse model of PD (4). Additionally, our real-time PCR and ELISA data showed that activation of CB_1 receptor attenuated the MPTP-induced increase in IL-1β and TNF-α in the SN. This action was reversed by CB_1 receptor antagonists, suggesting that CB_1 receptor-mediated anti-inflammatory actions contribute to its neuroprotective effect.

Notably, TH immunostaining experiments disclosed that WIN55,212-2 and HU210 failed to protect DA neurons from MPP^+ neurotoxicity in neuron-enriched mesencephalic cultures. This finding suggests that WIN55,212-2 and HU210 do not act by blocking MPP^+ entry into DA neurons. Although direct tests are yet to be performed, the results collectively provide indirect evidence that the neuroprotective effects of WIN55,212-2 and HU210 are not related to the prevention of MPP^+-induced inhibition of mitochondrial activity. However, these agents clearly exerted neuroprotective activity in cocultures of mesencephalic microglia and neurons, providing further evidence of their requirement for microglia. This result is supported by a previous report showing that HU210 reduces 6-OHDA–induced cerebellar granule neuronal death in conditioned media from mixed glial cell cultures (37). However, at the dose used in our experiments, HU210 (1 μM) suppressed neuronal cell death caused by 6-OHDA

Downloaded from http://journals.aai.org/jimmunol/article-pdf/187/12/6508/1342902/1102435.pdf by guest on 19 April 2024

in cultured mouse cerebellar granule cells devoid of microglia, as assessed using the Live and Dead assay. The apparent discrepancy between the results obtained from these two studies may be attributed to differences in toxin (MPP^+ versus 6-OHDA) and cell types (rat mesencephalic neurons versus mouse cerebellar granule neurons).

In this study, we have shown that WIN55,212-2 and Hu210 prevent DA neuronal death in the MPTP model of PD through inhibition of microglial activation, which can be reversed by CB_1 receptor selective antagonists AM251 and SR14716A, clearly indicative of CB_1 receptor involvement. However, these results may be irrelevant for CB_1 receptor-independent neuroprotection in the MPTP model (42). WIN55,212-2 rescued nigrostriatal DA neurons and inhibited microglial activation in CB_1 receptor knockout mice treated with MPTP, indicating CB_1 receptor-independent activity. The inconsistent experimental results between the two studies are probably a result of the different methods used for CB_1 receptor inhibition (genetic ablation of CB_1 receptor versus pharmacological inhibition) and varying drug doses (20 μg/kg versus 4 mg/kg) of WIN55,212-2. Alternatively, MPTP metabolism (conversion of MPTP into MPP^+) may be altered in CB_1 receptor knockout mice, compared with their wild-type counterparts, because MPTP-induced neurotoxicity is significantly lower in CB_1 receptor knockout mice (42).

Interestingly, Price and colleagues (42) showed that WIN55,212-2 prevented MPTP neurotoxicity on DA neurons through inhibition of microglial activation. These results were reversed by treatment with cannabinoid receptor type 2 (CB_2) receptor antagonist JTE in MPTP-treated mice, indicating possible involvement of microglial CB_2 receptor. This is in accordance with our unpublished observations that CB_2 receptor antagonist AM630 inhibited neuroprotective and anti-inflammatory effects of selective CB_2 receptor agonist JWH-133 in MPTP-treated mice (data not shown). These results cannot necessarily rule out the possibilities that activation of CB_2 receptor, at least in part, participates in DA neuronal survival through inhibition of microglial activation in MPTP mouse model, although further studies are required to determine the underlying mechanisms.

The predominant biochemical change in the STR of PD patients and MPTP-treated mice is a decrease in the dopamine level (2, 71). Such deficits in striatal dopamine in MPTP-treated mice lead to decreased latency to fall on an accelerating rotarod apparatus, reflecting diminished coordination and balance (4, 5). This finding is in keeping with the present biochemical and behavioral evidence that MPTP induces depletion of dopamine in the STR, with resultant motor dysfunction. Importantly, activation of the CB_1 receptor increased the striatal dopamine levels and ameliorated MPTP-induced motor deficits. These behavioral and in vivo biochemical effects of CB_1 receptor on the lesioned nigrostriatal DA system, together with the finding that activation of the CB_1 receptor inhibits microglial activation-mediated oxidative stress, suggest that the CB_1 receptor is a useful pharmacological target for treating PD and other disorders associated with neuroinflammation and microglia-derived oxidative damage.

Disclosures

The authors have no financial conflicts of interest.

References

1. Olanow, C. W., and W. G. Tatton. 1999. Etiology and pathogenesis of Parkinson's disease. *Annu. Rev. Neurosci.* 22: 123–144.
2. Savitt, J. M., V. L. Dawson, and T. M. Dawson. 2006. Diagnosis and treatment of Parkinson disease: molecules to medicine. *J. Clin. Invest.* 116: 1744–1754.
3. Hirsch, E. C., and S. Hunot. 2009. Neuroinflammation in Parkinson's disease: a target for neuroprotection? *Lancet Neurol.* 8: 382–397.
4. Chung, Y. C., S. R. Kim, and B. K. Jin. 2010. Paroxetine prevents loss of nigrostriatal dopaminergic neurons by inhibiting brain inflammation and oxidative stress in an experimental model of Parkinson's disease. *J. Immunol.* 185: 1230–1237.
5. Chung, Y. C., S. R. Kim, J. Y. Park, E. S. Chung, K. W. Park, S. Y. Won, E. Bok, M. Jin, E. S. Park, S. H. Yoon, et al. 2011. Fluoxetine prevents MPTP-induced loss of dopaminergic neurons by inhibiting microglial activation. *Neuropharmacology* 60: 963–974.
6. Liberatore, G. T., V. Jackson-Lewis, S. Vukosavic, A. S. Mandir, M. Vila, W. G. McAuliffe, V. L. Dawson, T. M. Dawson, and S. Przedborski. 1999. Inducible nitric oxide synthase stimulates dopaminergic neurodegeneration in the MPTP model of Parkinson disease. *Nat. Med.* 5: 1403–1409.
7. Wu, D. C., P. Teismann, K. Tieu, M. Vila, V. Jackson-Lewis, H. Ischiropoulos, and S. Przedborski. 2003. NADPH oxidase mediates oxidative stress in the 1-methyl-4-phenyl-1,2,3,6-tetrahydropyridine model of Parkinson's disease. *Proc. Natl. Acad. Sci. USA* 100: 6145–6150.
8. Mogi, M., M. Harada, H. Narabayashi, H. Inagaki, M. Minami, and T. Nagatsu. 1996. Interleukin (IL)-1 beta, IL-2, IL-4, IL-6 and transforming growth factor-alpha levels are elevated in ventricular cerebrospinal fluid in juvenile parkinsonism and Parkinson's disease. *Neurosci. Lett.* 211: 13–16.
9. Hirsch, E. C., S. Hunot, P. Damier, and B. Faucheux. 1998. Glial cells and inflammation in Parkinson's disease: a role in neurodegeneration? *Ann. Neurol.* 44 (Suppl 1): S115–S120.
10. Ferger, B., A. Leng, A. Mura, B. Hengerer, and J. Feldon. 2004. Genetic ablation of tumor necrosis factor-alpha (TNF-alpha) and pharmacological inhibition of TNF-synthesis attenuates MPTP toxicity in mouse striatum. *J. Neurochem.* 89: 822–833.
11. Pott Godoy, M. C., R. Tarelli, C. C. Ferrari, M. I. Sarchi, and F. J. Pitossi. 2008. Central and systemic IL-1 exacerbates neurodegeneration and motor symptoms in a model of Parkinson's disease. *Brain* 131: 1880–1894.
12. Matsuda, L. A., S. J. Lolait, M. J. Brownstein, A. C. Young, and T. I. Bonner. 1990. Structure of a cannabinoid receptor and functional expression of the cloned cDNA. *Nature* 346: 561–564.
13. Munro, S., K. L. Thomas, and M. Abu-Shaar. 1993. Molecular characterization of a peripheral receptor for cannabinoids. *Nature* 365: 61–65.
14. Chaperon, F., and M. H. Thiébot. 1999. Behavioral effects of cannabinoid agents in animals. *Crit. Rev. Neurobiol.* 13: 243–281.
15. Kim, S. R., D. Y. Lee, E. S. Chung, U. T. Oh, S. U. Kim, and B. K. Jin. 2005. Transient receptor potential vanilloid subtype 1 mediates cell death of mesencephalic dopaminergic neurons in vivo and in vitro. *J. Neurosci.* 25: 662–671.
16. Walter, L., A. Franklin, A. Witting, C. Wade, Y. Xie, G. Kunos, K. Mackie, and N. Stella. 2003. Nonpsychotropic cannabinoid receptors regulate microglial cell migration. *J. Neurosci.* 23: 1398–1405.
17. Bouaboula, M., B. Bourrié, M. Rinaldi-Carmona, D. Shire, G. Le Fur, and P. Casellas. 1995. Stimulation of cannabinoid receptor CB1 induces krox-24 expression in human astrocytoma cells. *J. Biol. Chem.* 270: 13973–13980.
18. Sánchez, C., I. Galve-Roperh, C. Canova, P. Brachet, and M. Guzmán. 1998. Delta9-tetrahydrocannabinol induces apoptosis in C6 glioma cells. *FEBS Lett.* 436: 6–10.
19. Molina-Holgado, E., J. M. Vela, A. Arévalo-Martín, G. Almazán, F. Molina-Holgado, J. Borrell, and C. Guaza. 2002. Cannabinoids promote oligodendrocyte progenitor survival: involvement of cannabinoid receptors and phosphatidylinositol-3 kinase/Akt signaling. *J. Neurosci.* 22: 9742–9753.
20. Devane, W. A., L. Hanus, A. Breuer, R. G. Pertwee, L. A. Stevenson, G. Griffin, D. Gibson, A. Mandelbaum, A. Etinger, and R. Mechoulam. 1992. Isolation and structure of a brain constituent that binds to the cannabinoid receptor. *Science* 258: 1946–1949.
21. Mechoulam, R., E. Fride, and V. Di Marzo. 1998. Endocannabinoids. *Eur. J. Pharmacol.* 359: 1–18.
22. Sugiura, T., S. Kondo, A. Sukagawa, S. Nakane, A. Shinoda, K. Itoh, A. Yamashita, and K. Waku. 1995. 2-Arachidonoylglycerol: a possible endogenous cannabinoid receptor ligand in brain. *Biochem. Biophys. Res. Commun.* 215: 89–97.
23. De Petrocellis, L., D. Melck, A. Palmisano, T. Bisogno, C. Laezza, M. Bifulco, and V. Di Marzo. 1998. The endogenous cannabinoid anandamide inhibits human breast cancer cell proliferation. *Proc. Natl. Acad. Sci. USA* 95: 8375–8380.
24. Pop, E. 1999. Cannabinoids, endogenous ligands and synthetic analogs. *Curr. Opin. Chem. Biol.* 3: 418–425.
25. Sarfaraz, S., F. Afaq, V. M. Adhami, and H. Mukhtar. 2005. Cannabinoid receptor as a novel target for the treatment of prostate cancer. *Cancer Res.* 65: 1635–1641.
26. Cannizzaro, C., M. D'Amico, P. Preziosi, and M. Martire. 2006. Presynaptic effects of anandamide and WIN55,212-2 on glutamatergic nerve endings isolated from rat hippocampus. *Neurochem. Int.* 48: 159–165.
27. Mackie, K. 2005. Distribution of cannabinoid receptors in the central and peripheral nervous system. *Handb. Exp. Pharmacol.* 168: 299–325.
28. Cristino, L., L. de Petrocellis, G. Pryce, D. Baker, V. Guglielmotti, and V. Di Marzo. 2006. Immunohistochemical localization of cannabinoid type 1 and vanilloid transient receptor potential vanilloid type 1 receptors in the mouse brain. *Neuroscience* 139: 1405–1415.
29. van der Stelt, M., W. B. Veldhuis, G. W. van Haaften, F. Fezza, T. Bisogno, P. R. Bar, G. A. Veldink, J. F. Vliegenthart, V. Di Marzo, and K. Nicolay. 2001. Exogenous anandamide protects rat brain against acute neuronal injury in vivo. *J. Neurosci.* 21: 8765–8771.
30. Docagne, F., V. Muñetón, D. Clemente, C. Ali, F. Loría, F. Correa, M. Hernangómez, L. Mestre, D. Vivien, and C. Guaza. 2007. Excitotoxicity in a chronic model of multiple sclerosis: Neuroprotective effects of cannabinoids through CB1 and CB2 receptor activation. *Mol. Cell. Neurosci.* 34: 551–561.

Downloaded from http://journals.aai.org/jimmunol/article-pdf/187/12/6508/1342902/1102435.pdf by guest on 19 April 2024

31. Melis, M., G. Pillolla, T. Bisogno, A. Minassi, S. Petrosino, S. Perra, A. L. Muntoni, B. Lutz, G. L. Gessa, G. Marsicano, et al. 2006. Protective activation of the endocannabinoid system during ischemia in dopamine neurons. *Neurobiol. Dis.* 24: 15–27.
32. González, S., C. Scorticati, M. García-Arencibia, R. de Miguel, J. A. Ramos, and J. Fernández-Ruiz. 2006. Effects of rimonabant, a selective cannabinoid CB1 receptor antagonist, in a rat model of Parkinson's disease. *Brain Res.* 1073-1074: 209–219.
33. Kelsey, J. E., O. Harris, and J. Cassin. 2009. The CB(1) antagonist rimonabant is adjunctively therapeutic as well as monotherapeutic in an animal model of Parkinson's disease. *Behav. Brain Res.* 203: 304–307.
34. Pisani, A., F. Fezza, S. Galati, N. Battista, S. Napolitano, A. Finazzi-Agrò, G. Bernardi, L. Brusa, M. Pierantozzi, P. Stanzione, and M. Maccarrone. 2005. High endogenous cannabinoid levels in the cerebrospinal fluid of untreated Parkinson's disease patients. *Ann. Neurol.* 57: 777–779.
35. Gubellini, P., B. Picconi, M. Bari, N. Battista, P. Calabresi, D. Centonze, G. Bernardi, A. Finazzi-Agrò, and M. Maccarrone. 2002. Experimental parkinsonism alters endocannabinoid degradation: implications for striatal glutamatergic transmission. *J. Neurosci.* 22: 6900–6907.
36. van der Stelt, M., S. H. Fox, M. Hill, A. R. Crossman, S. Petrosino, V. Di Marzo, and J. M. Brotchie. 2005. A role for endocannabinoids in the generation of parkinsonism and levodopa-induced dyskinesia in MPTP-lesioned non-human primate models of Parkinson's disease. *FASEB J.* 19: 1140–1142.
37. Lastres-Becker, I., F. Molina-Holgado, J. A. Ramos, R. Mechoulam, and J. Fernández-Ruiz. 2005. Cannabinoids provide neuroprotection against 6-hydroxydopamine toxicity in vivo and in vitro: relevance to Parkinson's disease. *Neurobiol. Dis.* 19: 96–107.
38. Lee, S., D. H. Kim, S. H. Yoon, and J. H. Ryu. 2009. Sub-chronic administration of rimonabant causes loss of antidepressive activity and decreases doublecortin immunoreactivity in the mouse hippocampus. *Neurosci. Lett.* 467: 111–116.
39. Ramírez, B. G., C. Blázquez, T. Gómez del Pulgar, M. Guzmán, and M. L. de Ceballos. 2005. Prevention of Alzheimer's disease pathology by cannabinoids: neuroprotection mediated by blockade of microglial activation. *J. Neurosci.* 25: 1904–1913.
40. West, M. J., L. Slomianka, and H. J. Gundersen. 1991. Unbiased stereological estimation of the total number of neurons in thesubdivisions of the rat hippocampus using the optical fractionator. *Anat. Rec.* 231: 482–497.
41. Przedborski, S., V. Jackson-Lewis, R. Djaldetti, G. Liberatore, M. Vila, S. Vukosavic, and G. Almer. 2000. The parkinsonian toxin MPTP: action and mechanism. *Restor. Neurol. Neurosci.* 16: 135–142.
42. Price, D. A., A. A. Martinez, A. Seillier, W. Koek, Y. Acosta, E. Fernandez, R. Strong, B. Lutz, G. Marsicano, J. L. Roberts, and A. Giuffrida. 2009. WIN55,212-2, a cannabinoid receptor agonist, protects against nigrostriatal cell loss in the 1-methyl-4-phenyl-1,2,3,6-tetrahydropyridine mouse model of Parkinson's disease. *Eur. J. Neurosci.* 29: 2177–2186.
43. Babior, B. M. 2004. NADPH oxidase. *Curr. Opin. Immunol.* 16: 42–47.
44. Cross, A. R., and A. W. Segal. 2004. The NADPH oxidase of professional phagocytes—prototype of the NOX electron transport chain systems. *Biochim. Biophys. Acta* 1657: 1–22.
45. Isobe, C., T. Abe, and Y. Terayama. 2010. Levels of reduced and oxidized coenzyme Q-10 and 8-hydroxy-2′-deoxyguanosine in the cerebrospinal fluid of patients with living Parkinson's disease demonstrate that mitochondrial oxidative damage and/or oxidative DNA damage contributes to the neurodegenerative process. *Neurosci. Lett.* 469: 159–163.
46. Alam, Z. I., S. E. Daniel, A. J. Lees, D. C. Marsden, P. Jenner, and B. Halliwell. 1997. A generalised increase in protein carbonyls in the brain in Parkinson's but not incidental Lewy body disease. *J. Neurochem.* 69: 1326–1329.
47. Beal, M. F. 1998. Excitotoxicity and nitric oxide in Parkinson's disease pathogenesis. *Ann. Neurol.* 44(Suppl 1): S110–S114.
48. Martín-Moreno, A. M., D. Reigada, B. G. Ramírez, R. Mechoulam, N. Innamorato, A. Cuadrado, and M. L. de Ceballos. 2011. Cannabidiol and other cannabinoids reduce microglial activation in vitro and in vivo: relevance to Alzheimer's disease. *Mol. Pharmacol.* 79: 964–973.
49. Centonze, D., A. Finazzi-Agrò, G. Bernardi, and M. Maccarrone. 2007. The endocannabinoid system in targeting inflammatory neurodegenerative diseases. *Trends Pharmacol. Sci.* 28: 180–187.
50. Kreitzer, A. C., and R. C. Malenka. 2007. Endocannabinoid-mediated rescue of striatal LTD and motor deficits in Parkinson's disease models. *Nature* 445: 643–647.
51. Fernandez-Ruiz, J., M. Moreno-Martet, C. Rodriguez-Cueto, C. Palomo-Garo, M. Gomez-Canas, S. Valdeolivas, C. Guaza, J. Romero, M. Guzman, R. Mechoulam, and J. A. Ramos. 2011. Prospects for cannabinoid therapies in basal ganglia disorders. *Br. J. Pharmacol.* 163: 1365–1378.
52. Morgese, M. G., T. Cassano, V. Cuomo, and A. Giuffrida. 2007. Anti-dyskinetic effects of cannabinoids in a rat model of Parkinson's disease: role of CB(1) and TRPV1 receptors. *Exp. Neurol.* 208: 110–119.
53. Sañudo-Peña, M. C., K. Tsou, and J. M. Walker. 1999. Motor actions of cannabinoids in the basal ganglia output nuclei. *Life Sci.* 65: 703–713.
54. Chevaleyre, V., K. A. Takahashi, and P. E. Castillo. 2006. Endocannabinoid-mediated synaptic plasticity in the CNS. *Annu. Rev. Neurosci.* 29: 37–76.
55. Piomelli, D. 2003. The molecular logic of endocannabinoid signalling. *Nat. Rev. Neurosci.* 4: 873–884.
56. Molina-Holgado, F., E. Pinteaux, J. D. Moore, E. Molina-Holgado, C. Guaza, R. M. Gibson, and N. J. Rothwell. 2003. Endogenous interleukin-1 receptor antagonist mediates anti-inflammatory and neuroprotective actions of cannabinoids in neurons and glia. *J. Neurosci.* 23: 6470–6474.
57. Sancho, R., M. A. Calzado, V. Di Marzo, G. Appendino, and E. Muñoz. 2003. Anandamide inhibits nuclear factor-kappaB activation through a cannabinoid receptor-independent pathway. *Mol. Pharmacol.* 63: 429–438.
58. Walter, L., and N. Stella. 2004. Cannabinoids and neuroinflammation. *Br. J. Pharmacol.* 141: 775–785.
59. Kim, S. U., and J. de Vellis. 2005. Microglia in health and disease. *J. Neurosci. Res.* 81: 302–313.
60. Block, M. L., L. Zecca, and J. S. Hong. 2007. Microglia-mediated neurotoxicity: uncovering the molecular mechanisms. *Nat. Rev. Neurosci.* 8: 57–69.
61. Beal, M. F. 2002. Oxidatively modified proteins in aging and disease. *Free Radic. Biol. Med.* 32: 797–803.
62. Fahn, S., and G. Cohen. 1992. The oxidant stress hypothesis in Parkinson's disease: evidence supporting it. *Ann. Neurol.* 32: 804–812.
63. Miller, R. L., M. James-Kracke, G. Y. Sun, and A. Y. Sun. 2009. Oxidative and inflammatory pathways in Parkinson's disease. *Neurochem. Res.* 34: 55–65.
64. Oyagi, A., Y. Oida, H. Hara, H. Izuta, M. Shimazawa, N. Matsunaga, T. Adachi, and H. Hara. 2008. Protective effects of SUN N8075, a novel agent with antioxidant properties, in in vitro and in vivo models of Parkinson's disease. *Brain Res.* 1214: 169–176.
65. Zhang, J., G. Perry, M. A. Smith, D. Robertson, S. J. Olson, D. G. Graham, and T. J. Montine. 1999. Parkinson's disease is associated with oxidative damage to cytoplasmic DNA and RNA in substantia nigra neurons. *Am. J. Pathol.* 154: 1423–1429.
66. Block, M. L., and J. S. Hong. 2007. Chronic microglial activation and progressive dopaminergic neurotoxicity. *Biochem. Soc. Trans.* 35: 1127–1132.
67. Gao, H. M., B. Liu, W. Zhang, and J. S. Hong. 2003. Critical role of microglial NADPH oxidase-derived free radicals in the in vitro MPTP model of Parkinson's disease. *FASEB J.* 17: 1954–1956.
68. Nagatsu, T., and M. Sawada. 2007. Biochemistry of postmortem brains in Parkinson's disease: historical overview and future prospects. *J. Neural Transm. Suppl.* 72: 113–120.
69. Zhao, C., Z. Ling, M. B. Newman, A. Bhatia, and P. M. Carvey. 2007. TNF-alpha knockout and minocycline treatment attenuates blood-brain barrier leakage in MPTP-treated mice. *Neurobiol. Dis.* 26: 36–46.
70. Teismann, P., K. Tieu, O. Cohen, D. K. Choi, D. C. Wu, D. Marks, M. Vila, V. Jackson-Lewis, and S. Przedborski. 2003. Pathogenic role of glial cells in Parkinson's disease. *Mov. Disord.* 18: 121–129.
71. Jackson-Lewis, V., and S. Przedborski. 2007. Protocol for the MPTP mouse model of Parkinson's disease. *Nat. Protoc.* 2: 141–151.

Downloaded from http://journals.aai.org/jimmunol/article-pdf/187/12/6508/1342902/1102435.pdf by guest on 19 April 2024